

## **Multi-source remote sensing data for natural habitat mapping in India**

Subhadeep Bhattacharjee, Solomon Gebremariam Tesfamichael

Department of Geography, Environmental Management & Energy Studies, University of Johannesburg, APK campus, Johannesburg, Auckland Park 2006, South Africa

subhadeepb@uj.ac.za

### **Abstract**

*Efficient mapping and monitoring of large spatial extents of the natural habitats are essential for nature conservation. The current study aimed to compare three open access remotely sensed data (Landsat-5 Thematic Mapper, Hyper Spectral Imager – HySI and Linear Imaging Self Scanning Sensor-III - LISS-III) to map the Land-Use Land-Cover (LULC) categories in and around Ranthambhore Tiger Reserve (RTR) of northwestern India. The Landsat-5 images were acquired in the pre-monsoon and post-monsoon seasons of 2011, while HySI and LISS-III images represented the pre-monsoon and post-monsoon seasons of 2011, respectively. Five land cover types including water bodies, bare soil / rock / sand, agricultural lands, open scrublands / grasslands and woodlands were created using Support Vector Machine (SVM) algorithm. The overall accuracy obtained from the HySI and LISS-III images were 67.5% and 79.1%. Landsat-5 yielded better accuracies for both the pre-monsoon and post-monsoon classified maps (77.6%). The spatial coverage of woodlands ranged from 13.6% to 20.4% while the spatial extent of the open scrublands / grasslands was estimated from 21.1% to 37.4% out of the total area of 3200 km<sup>2</sup>. Agricultural lands were the dominant land use type (ranging from 23.3% to 53.7% in spatial extent), whose progression could be a threat to other natural habitats and associated biodiversity. Therefore, future long-term studies are encouraged using such multiple data sources to assess the dynamics of natural habitats and other competing land cover types to understand the trend and level of threat that the natural habitats of this region in India are facing.*

*Keywords: HySI; Landsat; LISS-III; Ranthambhore Tiger Reserve; Remote sensing; Support Vector Machine.*

### **1. Introduction**

Biodiversity conservation can be managed effectively by periodic mapping of different habitat components (Morrison et al. 2012). Mapping of the natural habitats provides preemptive insights for the entire ecosystem conservation and better interpretation of various threats such as human induced changes in Land Use-Land Cover (LULC) patterns, alien species invasion, forest fire, soil erosion and climate change (Nagendra et al. 2013). Several studies utilized remote sensing algorithms for mapping the natural habitats to assess their historical and current conditions (e.g., Divíšek et al. 2014; Mochizuki et al. 2015; Harwood et al. 2016). Various remote sensing applications intended for nature conservation by natural habitat mapping have been documented in India as well (e.g., Kushwaha et al. 2000; Imam et al. 2012). Remote sensing techniques help in

acquisition and subsequent interpretation of the biophysical characteristics of the natural habitats to predict species distribution and abundance at regional or global scales (Mcdermid et al. 2005). Nagendra et al. (2013) suggested that remote sensing information should be acquired efficiently using multiple data sources to enable effective management of the Protected Areas.

For acquiring the surface information from multiple image statistics, Chander et al. (2008) conducted a comparative study on the observations of ground cover, tree canopy and impervious surface collected from Mesa, AZ and Salt Lake City, UT of USA. Information were acquired from five sensors - the high resolution Linear Imaging Self-Scanner-IV (LISS-IV), the medium resolution Linear Imaging Self-Scanner-III (LISS-III), the Advanced Wide-Field Sensor (AWiFS), Landsat-5 Thematic Mapper (TM) and Landsat-7 Enhanced TM Plus (ETM+). Similarly, Rahman and Saha (2009) studied spatial dynamics of cropland and cropping pattern change analysis in Bangladesh by comparing multi-temporal and multi-sensor Landsat TM and IRS P6 LISS III satellite images. In terms of improvement of remote sensing output, Benediktsson et al. (2012) suggested working with the multimodal data to accomplish research challenges.

However, remote sensing applications focusing on multiple open access data to help in natural habitat mapping in India is rare. Wani et al. (2010) discussed about the importance of using different variations (spatial, spectral, temporal, and radiometric resolutions) of remote sensing data for mapping various infrastructure and components of integrated watershed management. Nandy and Kushwaha (2011) classified and mapped the mangroves in Sunderban Biosphere Reserve (SBR), West Bengal, India using IRS 1D LISS-III data with different classification methodologies. In a different approach, Mehta and Agarwal (2012) attempted to retrieve Normalized Difference Vegetation Index (NDVI) as an indicator of biomass from Hyper-Spectral Imager (HySI) data by cross calibrating it with respect to Hyperion (Folkman et al. 2001). Yet, there was no previous study, which attempted to enumerate the spatial distribution of LULC categories in the northwestern Indian landscape by comparing multiple remote sensing data. Thus, the current study was carried out to map the spatial distribution of the natural habitats across the semi-arid landscape of Ranthambhore Tiger Reserve (RTR) and adjoining areas of northwestern India using multispectral and hyperspectral images obtained from three different remote sensing sources. We used field knowledge, space borne imagery and advanced machine learning techniques to produce the classified maps. Such a study has a great potential to provide decision makers with a statistically supported protocol, which can be adopted to monitor the ecological status of the entire region.

## **2. Methods**

### **2.1 Study Area**

RTR is located in the southeast part of Rajasthan State in the northwestern region of India and the total area of RTR is more than 1700 km<sup>2</sup> (Figure 1). The climate of RTR is typically sub-tropical dry climate having three distinct seasons – summer, winter and monsoon. Summer is very hot and continues from end of March to middle of July. The monsoon is generally from mid-July to

mid-September with the average rainfall of 750-800 mm (Reddy et al. 2002). The winter starts after rainy season from November and lasts until February. Elevation in the Reserve ranges from 200 m to 500 m above mean sea level. RTR is globally recognised for its endangered large felids - Royal Bengal tiger (*Panthera tigris*) and leopard (*Panthera pardus*).

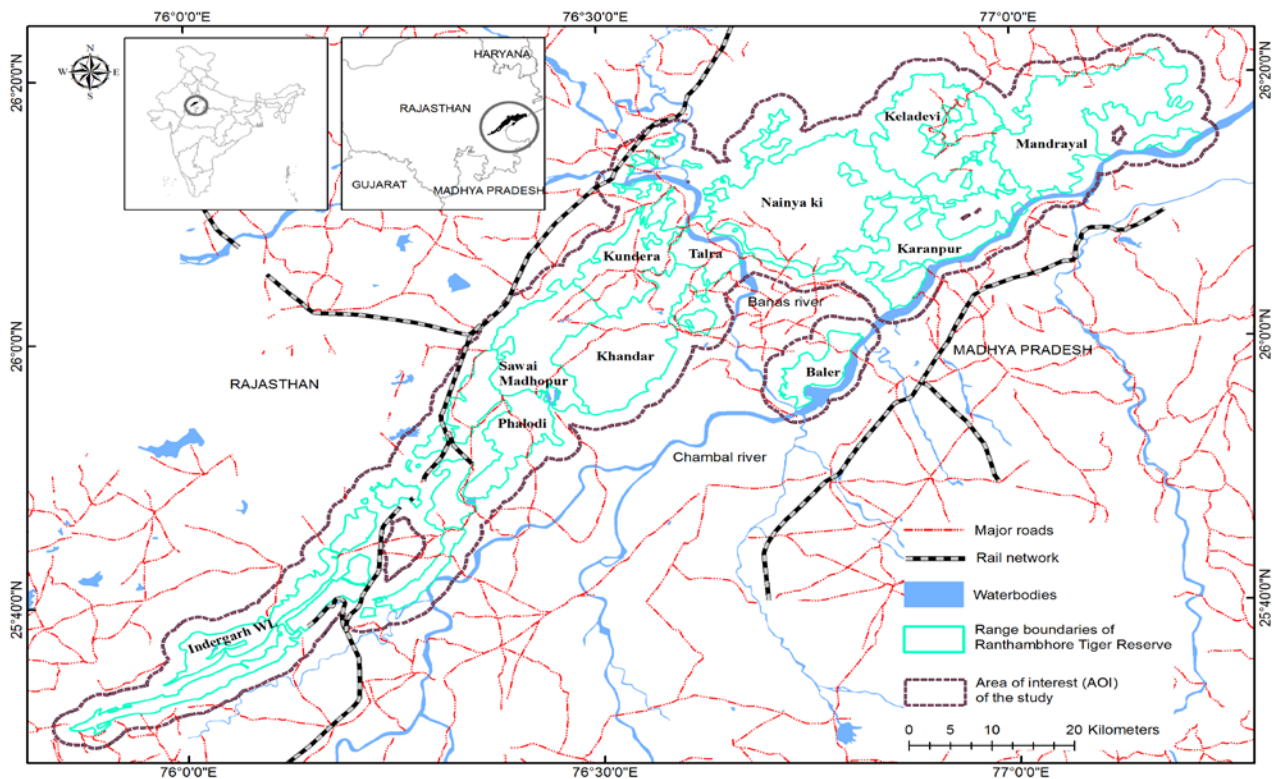


Figure 1. Ranthambhore Tiger Reserve (RTR) and the Area of Interest (AOI) of the study.

### 3. Remotely sensed data

The boundary coverage of RTR was obtained from the Rajasthan State Forest Department. A buffer of two kilometers was created around the Reserve to create the final area of interest (AOI – 3200 km<sup>2</sup>) as wildlife in India persisted their natural movements frequently up to 2 km out of the boundaries of the Protected Areas (Venkataraman, 2010). Four Landsat-5 Thematic Mapper images were acquired from the United States Geological Survey (USGS) online portal (<https://earthexplorer.usgs.gov>). Similarly, three HySI and 16 LISS-III images were obtained from the National Remote Sensing Centre (NRSC) of Indian Space Research Organization (ISRO) online portal (<http://bhuvan-noeda.nrsc.gov.in>). All these data are available to the public at no cost. These images were provided with geometric and terrain corrections while atmospheric correction was not needed as cloud-free images were selected for the current study. A summary of the remotely sensed images used in the study is provided in Table 1.

Table 1. Remotely sensed data used to map land cover types of RTR.

<b>Name of the sensor and vehicle</b>	<b>Image Acquisition Date (MMDDYYYY)</b>	<b>Bands used and their respective wavelengths</b>	<b>Spatial Resolution</b>	<b>Scene size (E-W x N-S)</b>
Landsat Thematic Mapper and Landsat -5	08.05.2011 <sup>#</sup> 15.05.2011 <sup>#</sup> 29.09.2011 <sup>\$</sup> 22.10.2011 <sup>\$</sup>	06 (blue: 0.44-0.52 $\mu\text{m}$ ; green: 0.52-0.60 $\mu\text{m}$ ; red: 0.63-0.69 $\mu\text{m}$ ; near infrared: 0.76-0.90 $\mu\text{m}$ ; shortwave infrared 1 (SWIR 1): 1.55-1.75 $\mu\text{m}$ and SWIR 2: 2.08-2.35 $\mu\text{m}$ )	30 m	183 km x 170 km
Hyper Spectral Imager – HySI and Indian Mini Satellite 1 or IMS 1	12.06.2011 <sup>#</sup> 12.06.2011 <sup>#</sup> 07.06.2011 <sup>#</sup>	17 (0.52 $\mu\text{m}$ ; 0.55 $\mu\text{m}$ ; 0.57 $\mu\text{m}$ ; 0.60 $\mu\text{m}$ ; 0.62 $\mu\text{m}$ ; 0.65 $\mu\text{m}$ ; 0.67 $\mu\text{m}$ ; 0.70 $\mu\text{m}$ ; 0.72 $\mu\text{m}$ ; 0.75 $\mu\text{m}$ ; 0.77 $\mu\text{m}$ ; 0.80 $\mu\text{m}$ ; 0.82 $\mu\text{m}$ ; 0.85 $\mu\text{m}$ ; 0.87 $\mu\text{m}$ ; 0.90 $\mu\text{m}$ and 0.92 $\mu\text{m}$ )	506 m	120 km x 140 km
Linear Imaging Self Scanning Sensor-III or LISS-III and Resourcesat-1	13.11.2011 <sup>\$</sup> 13.11.2011 <sup>\$</sup> 13.11.2011 <sup>\$</sup> 13.11.2011 <sup>\$</sup> 13.11.2011 <sup>\$</sup> 01.10.2011 <sup>\$</sup> 02.12.2011 <sup>\$</sup> 02.12.2011 <sup>\$</sup> 13.11.2011 <sup>\$</sup> 13.11.2011 <sup>\$</sup> 13.11.2011 <sup>\$</sup> 13.11.2011 <sup>\$</sup> 13.11.2011 <sup>\$</sup> 13.11.2011 <sup>\$</sup> 13.11.2011 <sup>\$</sup>	04 (0.52-0.59 $\mu\text{m}$ ; 0.62-0.68 $\mu\text{m}$ ; 0.77-0.86 $\mu\text{m}$ ; 1.55-1.70 $\mu\text{m}$ )	23.5 m	26 km x 29 km

<sup>#</sup>: pre-monsoon season and <sup>\$</sup>: post-monsoon season

#### **4. Image analysis**

Based on knowledge of the study area, we chose five LULC categories to describe our AOI – water bodies, bare soil / sand / rock, agricultural lands, open scrublands / grasslands and woodlands. These five broad classes covered almost the entire spatial extent of the AOI. Water bodies included natural and artificial water sources such as rivers, lakes, ponds, dams, ditches, canals and channels, which were covered with water for most of the year. Category of bare soil / sand / rock consisted of dry riverbeds, degraded areas with no vegetation, built up areas and barren rocky surfaces. Agricultural lands were associated to all farmlands, orchards and croplands. Open scrublands / grasslands were the areas covered with different shrubs, grasses and less than 10% of woody trees. Woodlands included northern tropical dry deciduous forests of *Anogeissus pendula* (Champion and Seth, 1968) and other associated woody species (*Acacia*, *Zizyphus*, *Butea*) as well as thickets of the invasive species *Prosopis juliflora*.

Guided by the thorough knowledge of the study area and visual interpretation of the LISS-III and Landsat multispectral images, a single training set was developed for a specific LULC class containing eight to ten pure pixels. Ten such training sets for each chosen LULC category were compiled for each image. These training sets served as inputs for classification using Support Vector Machine (SVM) algorithm. Choosing this classifier was advantageous as it followed non-parametric rules and it belonged to the supervised classification family, which required training data containing categories of interest as an initial input. SVM algorithms classify data such as spectral values in a Landsat imagery into LULC types by drawing vectors (hyperplanes) between nearest points of LULC classes (Boser et al. 1992; Vapnik, 1995; Vapnik, 1999). Another important feature of SVM, is that it assigns a class name to all samples that fall on one side of the vector. The classification was carried out using ArcGIS (ESRI® ArcGIS Desktop version 10.5, Redlands, California, USA). Similar specification such as the maximum number of samples used in the SVM classification was enforced for all the data.

#### **5. Accuracy assessment**

Stratified random sampling was opted to generate two sets of 513 accuracy assessment sampling points covering the entire AOI for pre and post monsoon seasons. A buffer of 45 m radius was created around each of these sampling points. A majority rule was applied to extract the most common LULC category within each buffer and they were subsequently plotted on Google Earth™ (<http://earth.google.com>) image within acceptable time window relative to all the image acquisition dates (a maximum of 30 days difference but in most cases within 15 days). Google Earth images were used as a source of reference to evaluate classification accuracy of LULC categories due to its high spatial resolution suitable to identify fine details of the LULC types following previous studies (e.g., Schneider et al. 2009; Zurqani et al. 2018).

Classification accuracy was assessed using statistics including overall, producer's and user's accuracies as well as kappa coefficient (Lillesand and Kiefer, 2000; Congalton and Green, 2009).

Overall accuracy was quantified by dividing the total number of correctly classified buffer areas by the total number of buffer areas. Producer's accuracy was computed by dividing the number of correctly classified buffer areas in each category by the number of buffer areas for that category in the reference data while the user's accuracies were calculated by dividing the number of correctly classified buffer areas in each category by the total number of buffer areas classified in that category. Kappa coefficient ( $\hat{k}$ , Equation 1) measured as the difference amongst the actual agreement between reference data and the automated classifier with the chance agreement between the reference data and a random classifier (Lillesand and Kiefer, 2000; Congalton and Green, 2009).

$$\hat{k} = \frac{N \sum_{i=1}^r x_{ii} - \sum_{i=1}^r (x_{i+} \times x_{+i})}{N^2 - \sum_{i=1}^r (x_{i+} \times x_{+i})} \dots\dots\dots\text{Equation 1}$$

where, r = number of rows in the error matrix;  $x_{ii}$  = the number of observations in row i and column i (on the major diagonal);  $x_{i+}$  = total of observations in row i;  $x_{+i}$  = total of observations in column i; N = total number of observations included in the matrix.

## 6. Results

The overall accuracy and kappa coefficient ( $\hat{k}$ ) of classifying the LULC categories of the AOI based on both pre-monsoon (Table 2) and post-monsoon (Table 3) Landsat-5 images were 77.6% and 0.70, respectively. Similarly, the overall accuracy of classifying the HySI and LISS-III images were 67.5% (Table 2) and 79.1% (Table 3), respectively. The kappa coefficient ( $\hat{k}$ ) of classifying the HySI and LISS-III images were 0.57 and 0.72 following the similar order. The user's accuracies for waterbodies in the pre-monsoon Landsat image-based map (100%) was more than that of the post-monsoon Landsat image-based map (87.5%) while the producer's accuracy was better for the latter than for the former. The user's accuracies for "Open scrublands / grasslands" and "Woodlands" classes for HySI image-based map were quite high (74.8% and 82.4%, respectively) as well as the producer's accuracy for the "Bare soil / Rock / Sand" class (83.9%) of the same map. For pre-monsoon season, Landsat-5 image-based classification had better user's and producer's accuracies than HySI except two classes (woodlands for user's accuracy and bare soil / rock / sand for producer's accuracy). In contrast, for the post-monsoon maps, LISS-III image-based classification had better user's accuracies for three classes than Landsat-5 based classification. Similar trend was observed in that season for the producer's accuracies as well. However, for "Woodlands" and "Open scrublands / grasslands" categories, all the three image sources showed quite high and comparable user's and producer's accuracies.

Table 2. Confusion / error matrix for LandSat-5 and HySI images using SVM algorithm for the chosen LULC categories of RTR and adjoining areas during pre-monsoon season in 2011.

		Observed LULC					Total	User's accuracy (%)
		Water bodies	Bare soil / rock / sand	Agricultural lands	Open scrublands / grasslands	Woodlands		
Classified LULC	Water bodies	14 <sup>§</sup> 7 <sup>†</sup>	0 <sup>§</sup> 1 <sup>†</sup>	0 <sup>§</sup> 4 <sup>†</sup>	0 <sup>§</sup> 2 <sup>†</sup>	0 <sup>§</sup> 0 <sup>†</sup>	14 <sup>§</sup> 14 <sup>†</sup>	100.0 <sup>§</sup> 50.0 <sup>†</sup>
	Bare soil / rock / sand	0 <sup>§</sup> 2 <sup>†</sup>	63 <sup>§</sup> 73 <sup>†</sup>	8 <sup>§</sup> 25 <sup>†</sup>	2 <sup>§</sup> 12 <sup>†</sup>	1 <sup>§</sup> 8 <sup>†</sup>	74 <sup>§</sup> 120 <sup>†</sup>	85.1 <sup>§</sup> 60.8 <sup>†</sup>
	Agricultural lands	2 <sup>§</sup> 7 <sup>†</sup>	15 <sup>§</sup> 12 <sup>†</sup>	111 <sup>§</sup> 87 <sup>†</sup>	25 <sup>§</sup> 30 <sup>†</sup>	13 <sup>§</sup> 14 <sup>†</sup>	166 <sup>§</sup> 150 <sup>†</sup>	66.9 <sup>§</sup> 58.0 <sup>†</sup>
	Open scrublands / grasslands	0 <sup>§</sup> 1 <sup>†</sup>	3 <sup>§</sup> 1 <sup>†</sup>	13 <sup>§</sup> 14 <sup>†</sup>	109 <sup>§</sup> 95 <sup>†</sup>	7 <sup>§</sup> 16 <sup>†</sup>	132 <sup>§</sup> 127 <sup>†</sup>	82.6 <sup>§</sup> 74.8 <sup>†</sup>
	Woodlands	1 <sup>§</sup> 0 <sup>†</sup>	6 <sup>§</sup> 0 <sup>†</sup>	4 <sup>§</sup> 6 <sup>†</sup>	15 <sup>§</sup> 12 <sup>†</sup>	101 <sup>§</sup> 84 <sup>†</sup>	127 <sup>§</sup> 102 <sup>†</sup>	79.5 <sup>§</sup> 82.4 <sup>†</sup>
	<b>Total</b>	17 <sup>§</sup> 17 <sup>†</sup>	87 <sup>§</sup> 87 <sup>†</sup>	136 <sup>§</sup> 136 <sup>†</sup>	151 <sup>§</sup> 151 <sup>†</sup>	122 <sup>§</sup> 122 <sup>†</sup>	513 <sup>§</sup> 513 <sup>†</sup>	
Producer's accuracy (%)		82.5 <sup>§</sup> 41.2 <sup>†</sup>	72.4 <sup>§</sup> 83.9 <sup>†</sup>	81.6 <sup>§</sup> 64.0 <sup>†</sup>	72.2 <sup>§</sup> 62.9 <sup>†</sup>	82.8 <sup>§</sup> 68.9 <sup>†</sup>		
Overall accuracy: 77.6% <sup>§</sup> and 67.5% <sup>†</sup>								
Kappa Coefficient (k): 0.70 <sup>§</sup> and 0.57 <sup>†</sup>								

Observed LULC: reference data interpreted from Google Earth image; §: results from LandSat-5 images; †: results from HySI images.

Table 3. Confusion / error matrix for LandSat-5 and LISS-III images using SVM algorithm for the chosen LULC categories of RTR and adjoining areas during post-monsoon season in 2011.

		Observed LULC					Total	User's accuracy (%)
		Water bodies	Bare soil / rock / sand	Agricultural lands	Open scrublands / grasslands	Woodlands		
Classified LULC	Water bodies	21 <sup>§</sup> 20 <sup>μ</sup>	1 <sup>§</sup> 0 <sup>μ</sup>	2 <sup>§</sup> 1 <sup>μ</sup>	0 <sup>§</sup> 0 <sup>μ</sup>	0 <sup>§</sup> 0 <sup>μ</sup>	24 <sup>§</sup> 21 <sup>μ</sup>	87.5 <sup>§</sup> 95.2 <sup>μ</sup>
	Bare soil / rock / sand	1 <sup>§</sup> 0 <sup>μ</sup>	43 <sup>§</sup> 49 <sup>μ</sup>	12 <sup>§</sup> 14 <sup>μ</sup>	3 <sup>§</sup> 6 <sup>μ</sup>	0 <sup>§</sup> 0 <sup>μ</sup>	59 <sup>§</sup> 69 <sup>μ</sup>	72.9 <sup>§</sup> 71.0 <sup>μ</sup>
	Agricultural lands	1 <sup>§</sup> 1 <sup>μ</sup>	14 <sup>§</sup> 3 <sup>μ</sup>	119 <sup>§</sup> 110 <sup>μ</sup>	40 <sup>§</sup> 22 <sup>μ</sup>	8 <sup>§</sup> 6 <sup>μ</sup>	182 <sup>§</sup> 142 <sup>μ</sup>	65.4 <sup>§</sup> 77.5 <sup>μ</sup>
	Open scrublands / grasslands	0 <sup>§</sup> 1 <sup>μ</sup>	2 <sup>§</sup> 6 <sup>μ</sup>	10 <sup>§</sup> 13 <sup>μ</sup>	138 <sup>§</sup> 149 <sup>μ</sup>	8 <sup>§</sup> 9 <sup>μ</sup>	158 <sup>§</sup> 178 <sup>μ</sup>	87.3 <sup>§</sup> 83.7 <sup>μ</sup>
	Woodlands	0 <sup>§</sup> 1 <sup>μ</sup>	0 <sup>§</sup> 2 <sup>μ</sup>	2 <sup>§</sup> 7 <sup>μ</sup>	11 <sup>§</sup> 15 <sup>μ</sup>	77 <sup>§</sup> 78 <sup>μ</sup>	90 <sup>§</sup> 103 <sup>μ</sup>	85.6 <sup>§</sup> 75.7 <sup>μ</sup>
	<b>Total</b>	23 <sup>§</sup> 23 <sup>μ</sup>	60 <sup>§</sup> 60 <sup>μ</sup>	145 <sup>§</sup> 145 <sup>μ</sup>	192 <sup>§</sup> 192 <sup>μ</sup>	93 <sup>§</sup> 93 <sup>μ</sup>	513 <sup>§</sup> 513 <sup>μ</sup>	
Producer's accuracy (%)		91.3 <sup>§</sup> 87.0 <sup>μ</sup>	71.7 <sup>§</sup> 81.7 <sup>μ</sup>	82.1 <sup>§</sup> 75.9 <sup>μ</sup>	71.9 <sup>§</sup> 77.6 <sup>μ</sup>	82.8 <sup>§</sup> 83.9 <sup>μ</sup>		
Overall accuracy: 77.6% <sup>§</sup> and 79.1% <sup>μ</sup>								
Kappa Coefficient (k): 0.70 <sup>§</sup> and 0.72 <sup>μ</sup>								

Observed LULC: reference data interpreted from Google Earth image; §: results from LandSat-5 images; †: results from HySI images.



The spatial distributions of the LULC classification based on the Landsat, HySI and LISS-III images are presented in Figure 2. In the northeast part of the AOI, the HySI (Figure 2B) and LISS-III (Figure 2D) images showed a large extent of open scrublands / grasslands juxtaposed between bare soil / rock / sand while Landsat based pre-monsoon (Figure 2A) and post-monsoon (Figure 2C) maps depicted that region mostly dominated with agricultural lands and bare soil / rock / sand categories. Landsat based maps showed larger spatial coverage by open scrublands / grasslands at the central to the south-west part of the AOI. Abundance of woodlands were visible at the central zone of AOI in all the maps. Difference in the waterbodies and agricultural lands during the pre and post monsoon seasons were quite distinct in the Landsat image-based maps. Figure 3 presents the spatial extents of the LULC classes created in the study. Landsat based maps showed spatial coverage of 13.6% to 17.1% for “woodlands” and 25.8% to 21.1% for “open scrublands / grasslands” in the pre and post monsoon seasons, respectively. HySI image-based maps showed lesser extent of spatial coverage by “woodlands” and “open scrublands / grasslands” than the LISS-III image-based maps. The spatial extents of the agricultural lands were estimated lowest in LISS-III image-based map and highest in post-monsoon Landsat map. Bare soil / rock / sand category showed highest extent in the HySI image-based map than other three maps. Extent of waterbodies did not vary much and were comparable in all the maps.

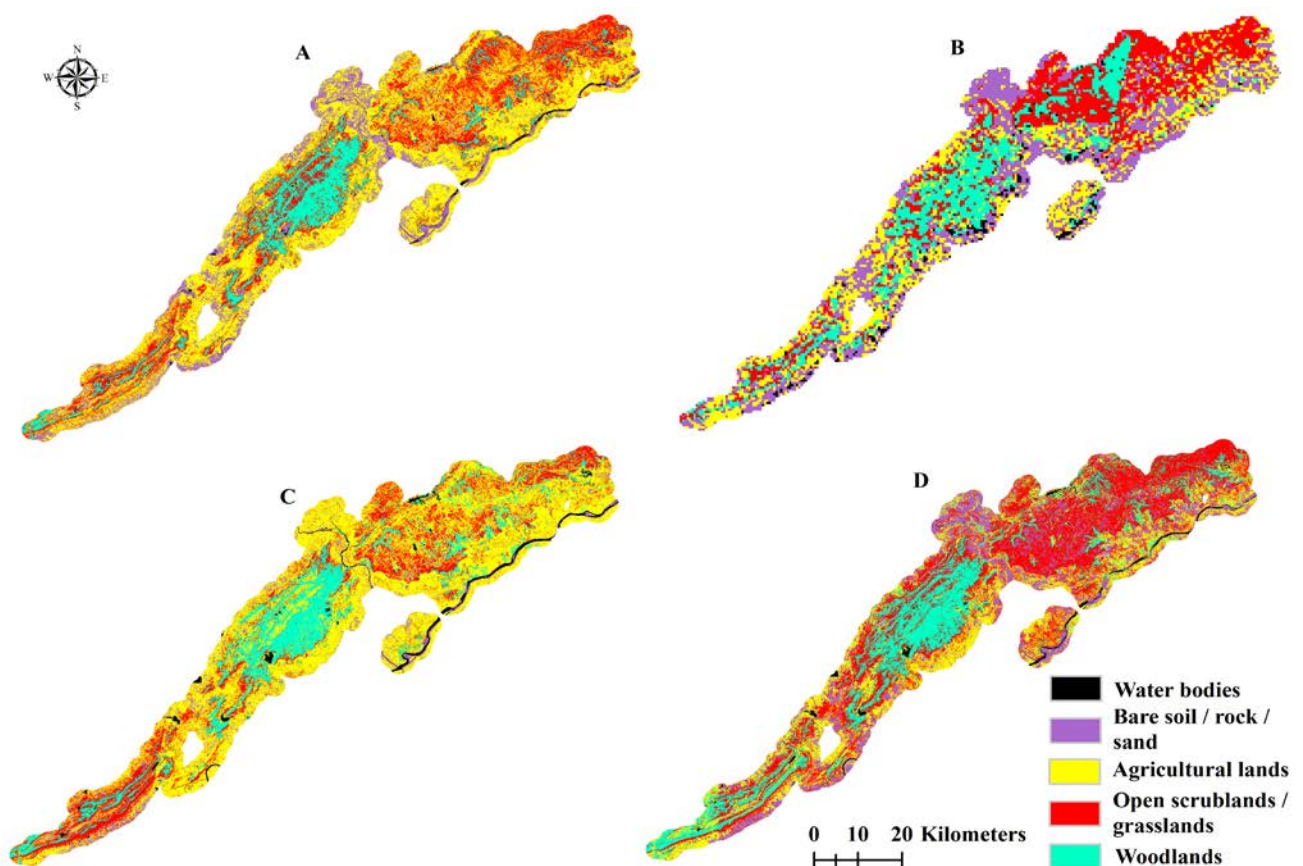


**Figure 2.** Classified land cover maps of RTR and adjoining 2 km buffer areas generated using SVM algorithm. Map A: pre-monsoon Landsat-5 image; Map B: pre-monsoon HySI image; Map C: post-monsoon Landsat-5 image and Map D: post-monsoon LISS-III image.



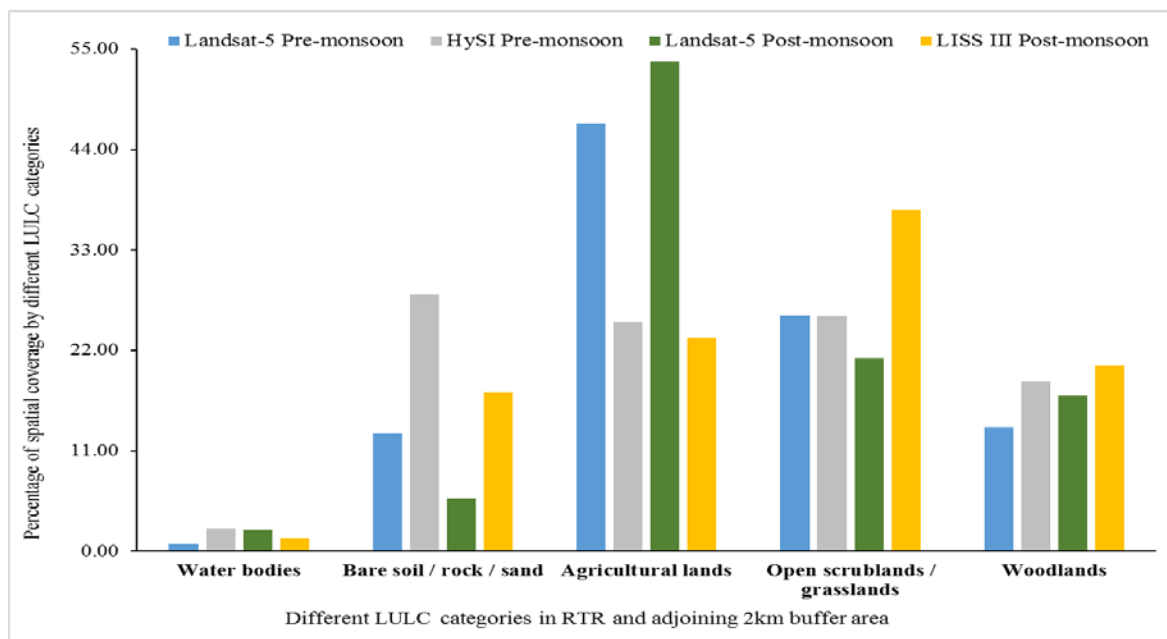


**Figure 3.** Comparative accounts of spatial coverage by different LULC categories from Landsat-5 (pre and post monsoon), HySI pre-monsoon and LISS-III post-monsoon classified maps.

## 7. Discussion

In the current study, amongst the pre-monsoon maps, majority of errors in LULC classification was observed between “agricultural lands” and “open scrublands / grasslands” classes for both Landsat and HySI data (Table 2). This observation is not surprising considering the month (May-June) in which the data were collected. Agriculture in this semi-arid region is mostly dependent on rainfall and during May-June, agricultural fields were not cultivated while the grasses dried out as well (Reddy et al. 2002). Thus, similar reflectance patterns by desiccated grasslands or open scrublands and uncultivated agricultural lands in the satellite images obtained in May-June contributed to the mis-classification. The overall accuracy for HySI image was quite low (67.5%) yet the user’s accuracies for both “open scrublands / grasslands” and “woodlands” produced from that same data were quite suitable (74.8% and 82.4%, respectively) for future application. The limitation of HySI image might be in the spatial resolution (506 m) but the higher spectral variation (17 bands) made it quite useful for accurately mapping these two natural habitats. Similarly, for LISS-III data, despite having higher spatial resolution than Landsat (23.5 m to 30 m), the user accuracies obtained for both “open scrublands / grasslands” and “woodlands” classes were lower than Landsat data (83.7% to 87.3% and 75.7% to 85.6%, respectively). Less spectral variation (4 bands to 6 bands of Landsat-5) could be a reason for this.

Another notable error was observed during pre-monsoon season when “open scrublands / grasslands” were mis-classified as “woodlands” resulting in low producer’s accuracy (72.2% and 62.9%) while the user’s accuracy was much higher (82.6% and 74.8%) for both the data sources (Table 2). Such high user’s accuracy would increase the probability for the management to identify “open scrublands / grasslands” on the ground following any of the classified maps. However, during

May-June, most of the *Anogeissus pendula* woodlands of RTR shed off their leaves (Reddy et al. 2002) and leafless branches most likely produced similar reflectance to the dried grassland / open scrublands (Yang and Prince, 1997). In addition, there were a few examples of mis-classification of woodlands as agricultural lands obtained during the pre-monsoon season. The artificially irrigated crops in the agricultural lands might have shown similar reflectance as the woodlands around the waterbodies, which retained green foliage even in the month of May-June.

The spatial coverage of woodlands estimated from all the images did not vary much (13.6% to 20.4%) while the spatial extent of open scrublands / grasslands varied greatly (21.1% to 37.4%). From the management point of view, it is safe to accept the conservative estimate of Landsat image (21.1%) so that considerable management efforts can be directed towards conserving this habitat. Inversely, potentially inflated information provided by LISS-III images on the 37.4% of available open scrublands / grasslands in AOI could hinder future policy decision to improve the spatial requirement of this habitat as it might be assumed as copious by the authorities. The open scrublands / grasslands located outside protected regime of the Tiger Reserve is highly vulnerable to fragmentation and irreversible land cover changes as showed by studies carried out in similar landscape matrix (Sadeghi et al. 2017). Therefore, the Protected Area authorities should ensure periodic monitoring of the spatial extent of grasslands / open scrublands and woodlands that are already existed within the Protected Area boundary, using timely and efficient techniques. To this effect, the findings obtained in the current study using Landsat-5, HySI and LISS-III images, which are freely available in public domain, are encouraging. The spatial resolution of 23.5 m to 30 m seemed reasonable to fulfill the objectives of the Protected Area management for monitoring a landscape of 3200 km<sup>2</sup> while HySI images were also quite significant in terms of mapping woodlands and open scrublands / grasslands. LISS-III sensor information post 2013 is not available and HySI information was only available for the year 2011. Initiatives to sustain these above-mentioned missions and thereafter making the information available in public domain would be helpful for the natural resource management in the entire country. Thus, we call for a repetitive mapping exercise of these natural habitats, as that would provide scientifically proven information to facilitate the monitoring of the spatial and temporal changes in all the LULC categories within and outside the Protected Areas.

## **8. Conclusions**

In this study, we mapped the distribution of natural habitats in and around RTR using three different remote sensing data for two seasons of 2011. The results showed that vast landscapes (3200 km<sup>2</sup>) could be classified into appropriate LULC categories with relatively high statistical accuracies. RTR and adjoining areas provide vital habitat for many endangered species on which they depend on. However, only 13.6% of woodlands and 21.1% of open scrubland / grassland in the entire AOI were estimated by this study, which might not be sufficient for the endangered

biodiversity. Thus, strategic initiatives should be continued to conserve and monitor this critical habitat using multiple datasets in order to ensure the ecological sustainability of the landscape.

## 9. Acknowledgements

We sincerely acknowledge Rajasthan State Forest Department in India. The Department of Geography, Environmental Management & Energy Studies (GEMES) and the Faculty of Science in the University of Johannesburg, South Africa is also cordially thanked for supporting the study.

## 10. References

- Benediktsson, J.A., Chanussot, J. and Moon, W.M. (2012). Very High-Resolution Remote Sensing: Challenges and Opportunities. *Proceedings of the IEEE*, 100: 1907-1910.
- Boser, B.E., Guyon, I.M. and Vapnik, V.N. (1992). A Training Algorithm for Optimal Margin Classifiers, in: *Proceedings of the Fifth Annual Workshop on Computational Learning Theory – COLT '92*, New York, USA: ACM Press, pp. 144-152.
- Champion, H.G. and Seth, S.K. (1968). *A revised survey of forest types of India*. Government of India, New Delhi.
- Chander, G., Coan, M.J. and Scaramuzza, P.L. (2008). Evaluation and Comparison of the IRS-P6 and the Landsat Sensors. *IEEE Transactions on Geoscience and Remote Sensing*, 46 (1): 209-221.
- Congalton, R.G. and Green, K. (2009). *Assessing the Accuracy of Remotely Sensed Data: Principles and Practices*. Second ed., CRC Press, Taylor and Francis Group, Boca Raton, Florida, United States of America.
- Divíšek, J., Zelený, D., Culek, M. and Št'astný, K. (2014). Natural habitats matter: Determinants of spatial pattern in the composition of animal assemblages of the Czech Republic. *Acta Oecologica*, 59: 7-17.
- Folkman, M., Pearlman, J., Liao, L. and Jarecke, P. (2001). EO-1/Hyperion hyperspectral imager design, development, characterization, and calibration. *Proceedings of SPIE*, 4151: 40-51.
- Harwood, T.D., Donohue, R.J., Williams, K.J., Ferrier, S., McVicar, T.R., Newell, G. and White, M. (2016). Habitat Condition Assessment System: a new way to assess the condition of natural habitats for terrestrial biodiversity across whole regions using remote sensing data. *Methods in Ecology and Evolution*, 7: 1050-1059.
- Imam, E., Hussain, T. and Mary, T. (2012). Modelling of Habitat Suitability Index for Muntjac (*Muntiacus muntjak*) Using Remote Sensing, GIS and Multiple Logistic Regression. *Journal of Settlements and Spatial Planning*, 3: 93-102.
- Kushwaha, S.P.S., Munkhtuya, S. and Roy, P.S. (2000). Geospatial modelling for goral habitat evaluation. *Journal of Indian Society of Remote Sensing*, 28: 293-303.
- Lillesand, T.M. and Kiefer, R.W. (2000). *Remote sensing and image interpretation*, fourth ed. NY: John Wiley and Sons Inc., New York.
- Mcdermid, G.J., Franklin, S.E. and LeDrew, E.F. (2005). Remote sensing for large-area habitat mapping. *Progress in Physical Geography*, 29 (4): 449-474.
- Mehta, M. and Agarwal, S. (2012). Cross-calibration of Indian Mini Satellite-1 HySI data using Hyperion: effect on Normalized Difference Vegetation Index. *Current Science*, 103 (5): 480-481.
- Mochizuki, S., Liu, D., Sekijima, T., Lu, J., Wang, C., Ozaki, K., Nagata, H., Murakami, T., Ueno, Y. and Yamagishi, S. (2015). Detecting the nesting suitability of the re-introduced Crested Ibis *Nipponia nippon* for nature restoration program in Japan. *Journal for Nature Conservation*, 28: 45-55.

- Morrison, M.L., Marcot, B.G. and Mannan, R.W. (2012). *Wildlife - Habitat Relationships - concepts and applications*, third ed. Island Press, Washington D.C.
- Nagendra, H., Lucas, R., Honrado, J.P., Jongman, R.H.G., Tarantino, C., Adamo, M. and Mairota, P. (2013). Remote sensing for conservation monitoring: Assessing protected areas, habitat extent, habitat condition, species diversity, and threats. *Ecological Indicators*, 33: 45-59.
- Nandy, S. and Kushwaha, S.P.S. (2011). Study on the utility of IRS 1D LISS-III data and the classification techniques for mapping of Sunderban mangroves. *Journal of Coast Conservation*, 15: 123-137.
- Rahman, Md. and Saha, S. (2009). Spatial dynamics of cropland and cropping pattern change analysis using Landsat TM and IRS P6 LISS III satellite images with GIS. *Geospatial Information Science*, 12 (2): 123-134.
- Reddy, G.V., Tyagi, R.K., Bhatnagar, D., Soni, R.G., Daima, M.L. and Sen, A. (2002). *Management plan of Ranthambhore Tiger Reserve (2002–2003 to 2011–2012)*, Rajasthan, India, State Forest Department.
- Sadeghi, M., Malekian, M. and Khodakarami, L. (2017). Forest losses and gains in Kurdistan province, western Iran: Where do we stand? *Egyptian Journal of Remote Sensing and Space Science*, 20: 51-59.
- Schneider, A., Friedl, M.A. and Potere, D. (2009). A new map of global urban extent from MODIS satellite data. *Environmental Research Letters*, 4, doi:10.1088/1748-9326/4/4/044003
- Vapnik, V.N. (1995). *The nature of statistical learning theory*, second ed. Springer Science + Business Media, New York.
- Vapnik, V.N. (1999). An overview of statistical learning theory. *IEEE Transactions on Neural Network*, 10: 988-999.
- Venkataraman, M. (2010). 'Site'ing the right reasons: critical evaluation of conservation planning for the Asiatic lion. *European Journal of Wildlife Research*, 56: 209-213.
- Wani, S.P., Roy, P.S., Rao, A.V.R.K., Barron, J., Ramachandran, K. and Balaji, V. (2010). *Application of new science tools in integrated watershed management for enhancing impacts*. Chapter 06 in S.P. Wani, J. Rockstrom and K.L. Sahrawat (eds.): *Integrated watershed management in rainfed agriculture*. pp: 159-204, CRC Press, Taylor and Francis, New York.
- Yang, J. and Prince, S.D. (1997). A theoretical assessment of the relation between woody canopy cover and red reflectance. *Remote Sensing of Environment*, 59 (3): 428-439.
- Zurqani, H. A., Posta, C.J., Mikhailova, E.A., Schlautman, M.A. and Sharp, J.L. (2018). Geospatial analysis of land use change in the Savannah River Basin using Google Earth Engine. *International Journal of Applied Earth Observation and Geoinformation*, 69: 175–185.